Multiple Orientation Acquisition to Invert Dipole Field for Quantitative Susceptibility Mapping

T. Liu[1,2], P. Spincemaille[2], L. de Rochefort[2], B. M. Kressler[1,2], and Y. Wang[1,2]

[1]Biomedical Engineering, Cornell University, Ithaca, NY, United States, [2]Radiology, Weill-Cornell Medical College, New York, NY, United States

Introduction

An important source of contrast in MRI is magnetic susceptibility [1], and its corresponding magnetic field can be mapped from the MR phase images. However, quantifying arbitrary susceptibility distributions by inverting the measured magnetic field remains challenging because it is intrinsically ill-posed. Some theoretical approaches have been proposed and remain to be validated experimentally [1] [2]. Here, we analyze the ill-posed problem and present a novel method to stabilize it by imaging the object at multiple orientations with respect to B_0. Preliminary data indicates that this multiple orientation approach stabilizes the inversion process and allows voxel-based susceptibility quantification.

Theory

In the presence of inhomogeneous susceptibility variations $\chi(\vec{r})$ within a uniform magnetic field $\overrightarrow{B_0} = B_0 \vec{z}$, the relative magnetic difference field (*RDF*) is given by the convolution [3] $RDF(\vec{r}) = B_z(\vec{r})/B_0 - 1 = FT^{-1}\left(1/3 - k_z^2/k^2\right) \otimes \chi(\vec{r})$, where B_z is the magnetic field component along $\vec{z}$, FT is the Fourier Transform, and k denotes components in the Fourier domain. Accordingly, the convolution kernel has zeros on a cone surface at the magic angle (54.7° from B_0). Therefore, directly inverting *RDF* to get $\chi(\vec{r})$ involves calculating $\left(1/3 - k_z^2/k^2\right)^{-1}$ on k-space, which is not defined at those zeros.

If the object is rotated N times with respect to B_0, an equivalent rotation of the *RDF* in the object frame is given by replacing $\left(1/3 - k_{axis}^2/k^2\right)$ in the previous expression, where k_{axis} is the rotated Fourier domain coordinates along B_0 with respect to the object. Then for each point X(k) in k-space, the following linear problem can be solved $\left[\left(1/3 - k_{axis1}^2/k^2\right),...,\left(1/3 - k_{axisN}^2/k^2\right)\right]^T \mathrm{X} = \left[FT(RDF_1),...,FT(RDF_N)\right]^T$. In an ideal environment without noise, if the number of orientations is greater than or equal to 3, then no more rank-deficiency exists for the system, except for k=0. In practice, the field measured from the signal phase has a non-homogeneous noise variance that is inversely proportional to the signal amplitude *S* [4]. In this situation, the following weighted linear system can be solved in image space to account for noise: $S \cdot RDF(\vec{r}) = S \cdot FT^{-1}\left(1/3 - k_{axis}^2/k^2\right) \otimes \chi(\vec{r})$.

Methods

A water phantom containing 7 test tubes (Fig. 1) was used. Tubes were filled with water for a reference scan, and then filled with different concentrations of gadolinium solutions. The experiment was conducted on a 1.5T GE Signa system using a standard 3D fast gradient echo. A 192*192*28 matrix size covered the entire phantom with an isotropic resolution of 0.5mm. Bandwidth was 62.50kHz, TR=50ms and flip angle 30° . 4 TE were used (3, 4, 5 and 6ms). The phantom was rotated in-plane 3 times by 120° increments. *RDF* maps were obtained by linear fitting the phase evolution as a function of echo time, and by subtracting the reference map. A dedicated registration algorithm based on best correlation search between intensity images (rotation/translation) was used to relocate the object with different orientations within the same frame ($\pm$0.5degree, $\pm$0.5 voxel size).

Both k-space direct inversion and image space iterative method were implemented. For direct inversion, *RDF* was additionally masked in the noisy air region to reduce noise influence. As an explicit inversion is not feasible for the image space method, an *LSQR* algorithm was used. To assess the precision of the proposed techniques, mean susceptibility values inside the tubes were measured and compared to the expected values.

Results

The measured *RDF* (Fig. 2) shows conspicuous dipolar pattern surrounding the tubes with different gadolinium concentrations and noisy region outside water dish. Both direct inversion and iterative method gave satisfactory images (Fig. 3 and 4). Different Gd concentrations were clearly resolved and no streaking artifacts were observed. While both methods gave linear results ($R^2 \approx 1$), the direct inversion was fast and tended to underestimate susceptibility, and the iterative method took several minutes and provided a good measurement of susceptibility (slope close to 1).

Discussion and Conclusion

An inversion technique based on imaging from multiple orientations was proposed to quantify arbitrary susceptibility distribution. Consistent susceptibility distributions were obtained with a good contrast. While sampling from more directions may lead to better inversion performance (data not shown), a minimum of 3 orientations is required to remove any rank-deficiency, otherwise no meaningful map was obtained. Nevertheless, a small underestimation was obtained that, besides experimental errors in the phantom preparation, could come from the limited information available (the field is not probed everywhere), misregistration, discretization or partial volume errors. The observed bias may be explained by the fact that k-space center is forced to be zero as every offset solution is suitable.

This technique could be used on small objects that can be rotated inside the bore or on open magnets. In addition, it may provide a simple tool for molecular and cellular or small animal imaging.

References

[1] Haacke et al., MRI: 23:1-25, 2005. [2] Li et al., MRM: 51:1077-82, 2004. [3] Salomir R, et al. Concept Magnetic Res: 19B:26-34, 2003. [4] Conturo, T.E. MRM: 15: 430-37, 1990

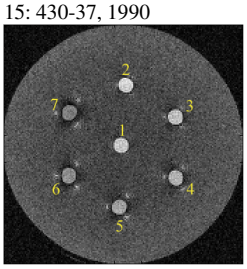

Fig.1. Phantom with Gd. Gd concentrations from #1 to #7 are 5mM to 35mM with 5mM increments.

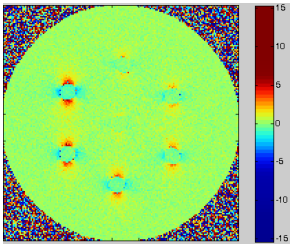

Fig. 2. One slice of RDF map. Unit in ppm

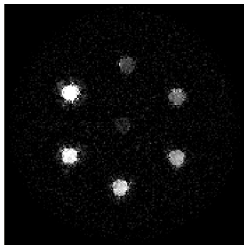

Fig. 3. Reconstruction from k-space direct inversion. Air region was set to zero for display purpose

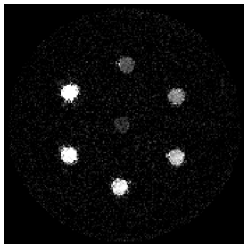

Fig. 4. Reconstruction from iterative method. Air region was set to zero for display purpose

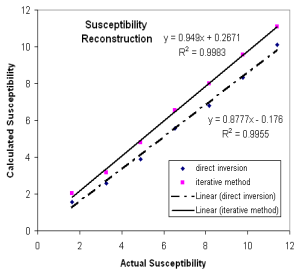

Fig. 5. Calculated susceptibilities versus actual susceptibilities.